



$B^0 \rightarrow D^0 \bar{D}^0 K^0$, $B^+ \rightarrow D^0 \bar{D}^0 K^+$, and the scalar $D\bar{D}$ bound state

L. R. Dai^{1,2,a}, Ju-Jun Xie^{3,4,b}, E. Oset^{2,3,c}

¹ Department of Physics, Liaoning Normal University, Dalian 116029, China

² Departamento de Física Teórica and IFIC, Centro Mixto Universidad de Valencia-CSIC, Institutos de Investigación de Paterna, Apartado 22085, 46071 Valencia, Spain

³ Institute of Modern Physics, Chinese Academy of Sciences, Lanzhou 730000, China

⁴ State Key Laboratory of Theoretical Physics, Institute of Theoretical Physics, Chinese Academy of Sciences, Beijing 100190, China

Received: 23 December 2015 / Accepted: 9 February 2016 / Published online: 4 March 2016
© The Author(s) 2016. This article is published with open access at Springerlink.com

Abstract We study the B^0 decay to $D^0 \bar{D}^0 K^0$ based on the chiral unitary approach, which generates the $X(3720)$ resonance, and we make predictions for the $D^0 \bar{D}^0$ invariant mass distribution. From the shape of the distribution, the existence of the resonance below threshold could be induced. We also predict the rate of production of the $X(3720)$ resonance to the $D^0 \bar{D}^0$ mass distribution with no free parameters.

1 Introduction

The weak decay of heavy hadrons has brought a wealth of information concerning the interaction of mesons, and mesons with baryons. In these reactions one finds mesons or mesons with baryons in the final state, some of which are subject to intense debate as regards their nature [1,2]. A recent review [3] on this subject has helped to clarify the situation and has shown the potential of these reactions to bring further light into this debate. The scalar meson sector is emblematic and the chiral unitary approach, unitarizing in coupled channels the information contained in the chiral Lagrangians [4], has shown that the $f_0(500)$, $f_0(980)$, $a_0(980)$ resonances appear as a consequence of the interaction of pseudoscalar mesons and respond to a kind of molecular structure of these components [5–10], diverting from the standard $q\bar{q}$ nature of most mesons. The case of the $f_0(500)$ (σ meson) has been thoroughly discussed in a recent review [11] and the situation has been much clarified. In this picture, the $f_0(980)$ stands as a bound $K\bar{K}$ state, with a small component of $\pi\pi$ that provides the decay channel of this state. Much before the advent of the chiral unitary approach, the $K\bar{K}$ molecular nature of the $f_0(980)$ had already been claimed [12]. A perspective

into these “extraordinary states” was also recently given in the Hadron2015 Conference by Jaffe [13].

The chiral Lagrangians can be obtained from a more general framework, which includes vector mesons, the local hidden gauge approach [14–17]. In this picture the chiral Lagrangians are obtained by exchanging vector mesons between the pseudoscalar mesons. This picture is most welcome because it allows us to extend the dynamics of the chiral Lagrangians to the heavy quark sector, and the interaction of $D\bar{D}$, for instance, would be given by the exchange of light vector mesons. Heavy vector mesons could also be exchanged, but their large mass makes the contributions of these terms subdominant, and the dominant terms, where the heavy quarks act as spectators [18,19], automatically satisfy the rules of heavy quark spin symmetry (HQSS) [20,21]. It is then not surprising that, in analogy to the $K\bar{K}$ interaction, which generates the $f_0(980)$, the $D\bar{D}$ interaction also gives rise to a bound state, which was studied in [22]. This state was also predicted in [23,24] using effective field theory that implements HQSS. In [25] the results of the $e^+e^- \rightarrow J/\psi D\bar{D}$ reaction close to threshold [26] were analyzed. A bump around the $D\bar{D}$ threshold was observed and the fit to the data was compatible with a state below threshold at 3720 MeV (we shall call this state $X(3720)$ from now on).

On the other hand, the study of B and D weak decays looking at resonances in the final state, or threshold behavior of invariant mass distributions, has shown that these reactions have a potential to tell us about the existence of “hidden” resonances and their nature. In this sense, in [27] a natural explanation was given, in terms of the $f_0(500)$, $f_0(980)$ as dynamically generated resonances [5,11], for the experimental facts that in the $B_s^0 \rightarrow J/\psi \pi^+\pi^-$ reaction the $f_0(980)$ was clearly observed and no trace of the $f_0(500)$ was seen [28], while in the case of the B^0 decay, the $f_0(500)$ was seen and only a minor fraction of the $f_0(980)$ was observed [29].

^a e-mail: dailr@lnnu.edu.cn

^b e-mail: xiejun@impcas.ac.cn

^c e-mail: oset@ific.uv.es

These results were complemented by the study of the D weak decays, were the production of $f_0(500)$, $f_0(980)$, and $a_0(980)$ were studied [30].

The idea in this paper will be to make predictions for the $D\bar{D}$ invariant mass distribution in the decay of B^0 . In this sense the work of [31], where the $B_s^0 \rightarrow D_s^-(KD)^+$ was studied, showed that from the spectrum of the KD invariant mass one could determine the existence of the D_{s0}^{*+} (2317) below threshold and the amount of the KD component in its wave function, using the compositeness sum rule of [32–35]. A similar work was also done in [36] where the reactions $\bar{B}^0 \rightarrow \bar{K}^{*0}X(YZ)$ and $\bar{B}_s^0 \rightarrow \phi X(YZ)$ with $X(4160)$, $Y(3940)$, $Z(3930)$ were studied. It was found there that from the study of $D^*\bar{D}^*$ and $D_s^*\bar{D}_s^*$ mass distributions close to threshold, the existence of resonances below threshold could be induced.

In the present paper we will study the B^0 decay to $D^0\bar{D}^0K^0$ with a model based on the work of [22] that generates the $X(3720)$ resonance, and that will make predictions for the $D^0\bar{D}^0$ invariant mass distribution. The theory predicts the shape of the distribution close to threshold, but not the absolute normalization. However, from the shape of the distribution the existence of the resonance below threshold could be induced. Additionally, we shall also evaluate the rate of production of the $X(3720)$ resonance, irrelevant of its decay channel, and we will show that the ratio of this rate to the $D^0\bar{D}^0$ mass distribution is then predicted with no free parameters, under the assumption that the $X(3720)$ resonance is dynamically generated. The implementation of the experiment would provide a boost in the search of this elusive state, which we think really exists. This experiment and related ones are currently under investigation by the LHCb Collaboration [37] and this gives us a motivation to perform the calculations at the present time. So far, the related experiment $B^+ \rightarrow D^0\bar{D}^0K^+$ has already been done [38]. The $D^0\bar{D}^0$ invariant mass is measured, but with very small statistics close to threshold. A sharp peak is identified, which corresponds to the excitation of the $\psi(3770)$ charmonium state, which decays in p-wave into $D^0\bar{D}^0$. The $X(3720)$ state is a scalar meson and it decays into $D^0\bar{D}^0$ in s-wave. In this sense, testing the invariant mass predicted here should require one to separate the s-wave from the p-wave part of the spectrum, something which is already currently been done by the partial wave analysis of the LHCb Collaboration, where the contribution of the ρ and $f_0(500)$ are separated in the B^0 decay to $J/\psi\pi^+\pi^-$ [29]. In any case, in the work of [38] the contribution of the $\psi(3770)$ is separated and this allows us to make a comparison of our results with this distribution. With present errors we find good agreement with the data, thus getting extra support for the $X(3720)$ state. However, our study indicates that the $B^0 \rightarrow D^0\bar{D}^0K^0$ reactions is better suited than the $B^+ \rightarrow D^0\bar{D}^0K^+$ one to give information on that state.

2 Formalism

If we followed the steps of Refs. [27, 39], a possible way for the $\bar{B}^0 \rightarrow D^0\bar{D}^0\bar{K}^0$ to proceed would be the following: in the first place we would produce a $c\bar{c}$ together with a $s\bar{d}$ pair as shown in Fig. 1.

The next step would consist in introducing a new $q\bar{q}$ state with the quantum numbers of the vacuum, $\bar{u}u + \bar{d}d + \bar{s}s + \bar{c}c$ in between the created $c\bar{c}$ pair, and in seeing which combinations of mesons appear. This is depicted in Fig. 2. This would lead to some $D\bar{D}\bar{K}^0$ components.

This way chosen to hadronize the quarks follows the path of [27, 30, 36, 39], based on the topology of the internal emission [40, 41]. However, in the present case, we also have external emission, which is color favored and, thus, we adhere to this other mechanism, which is depicted in Fig. 3 at the quark level (in Sect. 5 we will also consider the mechanism of Fig. 2). The hadronization is now done including a $q\bar{q}$ scalar

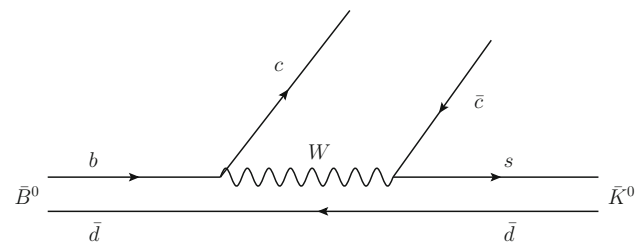


Fig. 1 Possible diagram at the quark level for \bar{B}^0 decays into $c\bar{c}$ and a $s\bar{d}$ pair

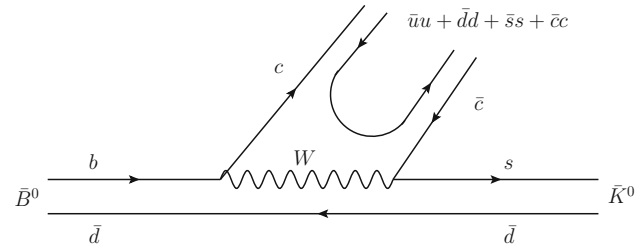


Fig. 2 Hadronization of the $c\bar{c}$ pair into two vector mesons for \bar{B}^0 decay

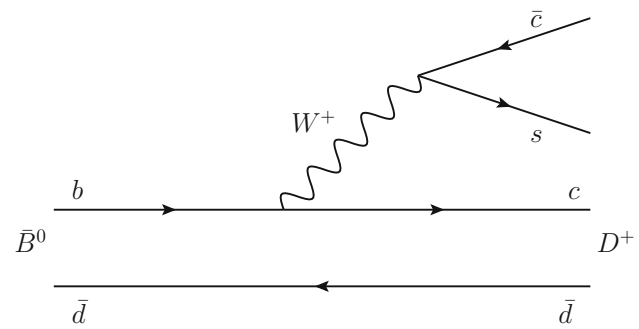


Fig. 3 Diagram at quark level for external emission of $s\bar{c}$ and $c\bar{d}$

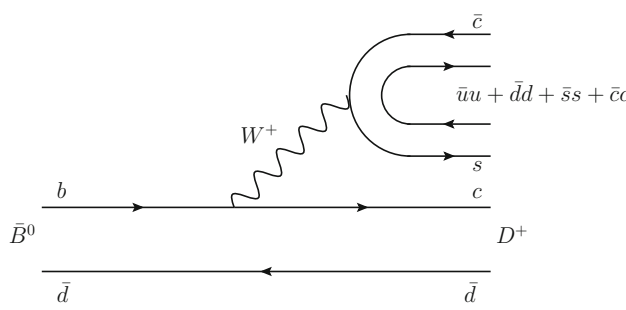


Fig. 4 The hadronization of the $s\bar{c}$ pair into two mesons

pair inside the $s\bar{c}$ pair, as shown in Fig. 4, and technically this is done as follows: an easy way to see which mesons are produced in the hadronization of $s\bar{c}$ is to introduce the $q\bar{q}$ matrix

$$M = \begin{pmatrix} u\bar{u} & u\bar{d} & u\bar{s} & u\bar{c} \\ d\bar{u} & d\bar{d} & d\bar{s} & d\bar{c} \\ s\bar{u} & s\bar{d} & s\bar{s} & s\bar{c} \\ c\bar{u} & c\bar{d} & c\bar{s} & c\bar{c} \end{pmatrix} = \begin{pmatrix} u \\ d \\ s \\ c \end{pmatrix} (\bar{u} \ \bar{d} \ \bar{s} \ \bar{c}). \quad (1)$$

In order to get the pair of mesons it is convenient to write the $q\bar{q}$ in terms of pseudoscalar mesons and then the M matrix has its equivalent matrix in ϕ given by

$$\phi = \begin{pmatrix} \frac{\eta}{\sqrt{3}} + \frac{\pi^0}{\sqrt{2}} + \frac{\eta'}{\sqrt{6}} & \pi^+ & K^+ & \bar{D}^0 \\ \pi^- & \frac{\eta}{\sqrt{3}} - \frac{\pi^0}{\sqrt{2}} + \frac{\eta'}{\sqrt{6}} & K^0 & D^- \\ K^- & \bar{K}^0 & \sqrt{\frac{2}{3}}\eta' - \frac{\eta}{\sqrt{3}} & D_s^- \\ D^0 & D^+ & D_s^+ & \eta_c \end{pmatrix}, \quad (2)$$

which incorporates the standard η , η' mixing [42]. Now we see that (see Refs. [31, 43])

$$\begin{aligned} M \cdot M &= \begin{pmatrix} u \\ d \\ s \\ c \end{pmatrix} (\bar{u} \ \bar{d} \ \bar{s} \ \bar{c}) \begin{pmatrix} u \\ d \\ s \\ c \end{pmatrix} (\bar{u} \ \bar{d} \ \bar{s} \ \bar{c}) \\ &= \begin{pmatrix} u \\ d \\ s \\ c \end{pmatrix} (\bar{u} \ \bar{d} \ \bar{s} \ \bar{c}) (\bar{u}u + \bar{d}d + \bar{s}s + \bar{c}c) \\ &= M(\bar{u}u + \bar{d}d + \bar{s}s + \bar{c}c). \end{aligned} \quad (3)$$

Thus, in terms of mesons, the hadronized $s\bar{c}$ pair will be given by

$$\begin{aligned} s\bar{c}(\bar{u}u + \bar{d}d + \bar{s}s + \bar{c}c) &\equiv (M \cdot M)_{34} \equiv (\phi \cdot \phi)_{34} \\ &= K^- \bar{D}^0 + \bar{K}^0 D^- + \left(\sqrt{\frac{2}{3}}\eta' - \frac{\eta}{\sqrt{3}} \right) D_s^- + D_s^- \eta_c. \end{aligned} \quad (4)$$

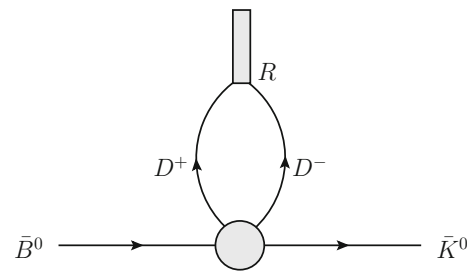


Fig. 5 Diagrammatic representation of the formation of the resonance R through rescattering of D^+D^- and coupling to the resonance

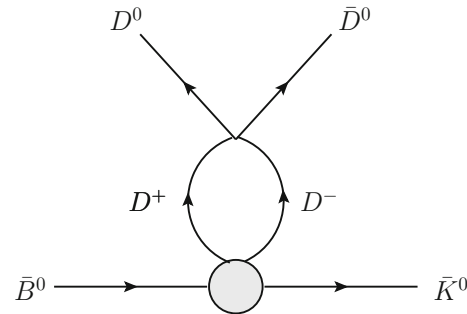


Fig. 6 Diagrammatic representation of the formation of the resonance R through rescattering of D^+D^- and coupling to $D^0\bar{D}^0$

We have the meson–meson components of Eq. (4), together with a D^+ of Fig. 3. If we want to have $D\bar{D}^0$ and \bar{K}^0 at the end, we must take the $\bar{K}^0 D^-$ component of Eq. (4) and let the D^+D^- interact to have $D\bar{D}^0$. Similarly, if we want to produce the scalar resonance $X(3720)$, which has zero charge, it is also the $\bar{K}^0 D^-$ component of Eq. (4) that we must take, and we will let the D^+D^- interact to give the resonance $X(3720)$ at the end. Hence, diagrammatically the latter process is depicted in Fig. 5. For the case of $D^0\bar{D}^0$ production the mechanism is depicted in Fig. 6.

Analytically we will now have

$$t(\bar{B}^0 \rightarrow \bar{K}^0 R) = V_P G_{D^+D^-} g_{R,D^+D^-}, \quad (5)$$

where $G_{M_1 M_2}$ is the loop function of the two intermediate meson propagators [5] and $g_{R,M_1 M_2}$ is the coupling of the resonance to the $M_1 M_2$ meson pair.

Taking into account that, with the doublets $(D^+, -D^0)$ and (\bar{D}^0, D^-) , the isospin $I = 0$ state of $D\bar{D}$ is

$$|I = 0, D\bar{D}\rangle = \frac{1}{\sqrt{2}}(D^+D^- + D^0\bar{D}^0), \quad (6)$$

Eq. (5) can be rewritten as

$$t(\bar{B}^0 \rightarrow \bar{K}^0 R) = V_P G_{D^+D^-} g_{R,D\bar{D}}^{I=0} \frac{1}{\sqrt{2}}. \quad (7)$$

The factor V_P entails the weak amplitudes plus the hadronization factors. We take it as a constant since we are only concerned about a restricted range of invariant masses, and the

factor prior to the final state interaction is smooth in that range [44, 45] (see section 3.3 of Ref. [3], for a more complete discussion of this issue and other approaches).

The partial decay width of $\bar{B}^0 \rightarrow \bar{K}^0 R$ decay will be

$$\Gamma_R = \frac{1}{8\pi} \frac{1}{M_{\bar{B}^0}^2} |t(\bar{B}^0 \rightarrow \bar{K}^0 R)|^2 p_{\bar{K}^0} \quad (8)$$

where $p_{\bar{K}^0}$ is the \bar{K}^0 momentum in the rest frame of the \bar{B}^0 .

3 Complementary test of the molecular nature of the resonances

In this section we make a test that is linked to the molecular nature of the resonances. We study the decay $\bar{B}^0 \rightarrow \bar{K}^0 D^0 \bar{D}^0$ close to the $D\bar{D}$ threshold depicted in Fig. 6.

The production matrix will be given by

$$t(\bar{B}^0 \rightarrow \bar{K}^0 D^0 \bar{D}^0) = V_P G_{D^+ D^-} t_{D^+ D^- \rightarrow D^0 \bar{D}^0} \quad (9)$$

We must evaluate the coupled channels $D^+ D^-$, $D^0 \bar{D}^0$, $D_S^+ D_s^-$ amplitudes which will contain $I = 0$ and $I = 1$, but close to the $D\bar{D}$ threshold they are dominated by $I = 0$ [the $I = 1$ is about 20 times smaller than that of $I = 0$, but we include it in Eq. (9) too]. The meson–meson loop function G and the scattering matrix $t_{i \rightarrow j}$ are evaluated following Ref. [22] as discussed later in the results section.

The differential cross section for production will be given by

$$\frac{d\Gamma}{dM_{\text{inv}}} = \frac{1}{32\pi^3} \frac{1}{M_{\bar{B}^0}^2} p_{\bar{K}^0} \tilde{p}_D |t(\bar{B}^0 \rightarrow \bar{K}^0 D^0 \bar{D}^0)|^2 \quad (10)$$

where $p_{\bar{K}^0}$ is the \bar{K}^0 momentum in the \bar{B}^0 rest frame and \tilde{p}_D the D momentum in the $D\bar{D}$ rest frame. By comparing this equation with Eq. (8) for the coalescence production of the resonance in $\bar{B}^0 \rightarrow \bar{K}^0 R$, we find

$$\begin{aligned} R_\Gamma &= \frac{M_R^3}{p_{\bar{K}^0} \tilde{p}_D} \frac{1}{\Gamma_R} \frac{d\Gamma}{dM_{\text{inv}}} \\ &= \frac{M_R^3}{4\pi^2} \frac{1}{p_{\bar{K}^0} (M_R)} \frac{|t(\bar{B}^0 \rightarrow \bar{K}^0 D^0 \bar{D}^0)|^2}{|t(\bar{B}^0 \rightarrow \bar{K}^0 R)|^2} \end{aligned} \quad (11)$$

where we have divided the ratio of widths by the phase space factor $p_{\bar{K}^0} \tilde{p}_D$ and multiplied by M_R^3 to get a constant value at threshold and a dimensionless magnitude. We apply this method for the $X(3720)$ resonance that couples strongly to $D\bar{D}$.

The results obtained are easily translated to the $B^- \rightarrow D^0 \bar{D}^0 K^-$ decay. The diagrams equivalent to Figs. 3, 4, 5 and 6, are now in Figs. 7, 8, 9 and 10. The situation is analogous to the former one, the hadronization of the $s\bar{c}$ pair proceeds in the same way as in Eq. (4), and the extra $c\bar{u}$ pair gives rise to a D^0 , unlike in the former case where the $c\bar{d}$ pair gave rise to a D^+ . Hence, from the $(K^- \bar{D}^0 + \bar{K}^0 D^-) D^0$ contribution

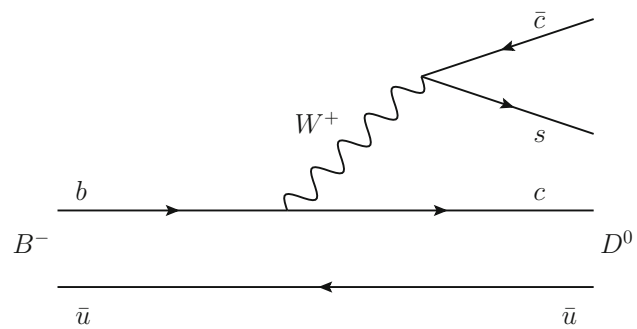


Fig. 7 The hadronization of the $s\bar{c}$ pair into two mesons

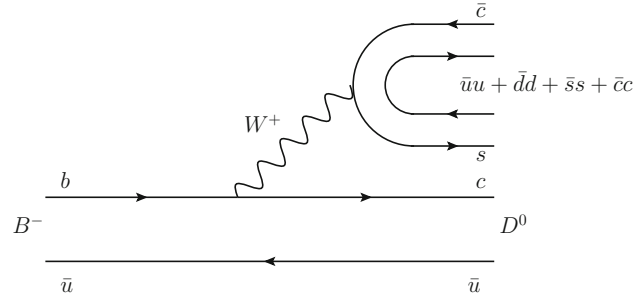


Fig. 8 The hadronization of the $s\bar{c}$ pair into two mesons

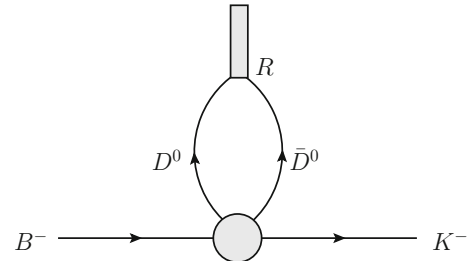


Fig. 9 Diagrammatic representation of the formation of the resonance R through rescattering of $D^0 \bar{D}^0$ and coupling to the resonance

at the primary step, we can already produce $K^- D^0 \bar{D}^0$ at tree level and the $D\bar{D}$ rescattering will be done by the $D^0 \bar{D}^0$ component.

Then the equation equivalent to Eqs. (7) and (9)

$$t(B^- \rightarrow K^- R) = V_P G_{D^0 \bar{D}^0} g_{R, D\bar{D}}^{I=0} \frac{1}{\sqrt{2}}, \quad (12)$$

$$t(B^- \rightarrow K^- D^0 \bar{D}^0) = V_P (1 + G_{D^0 \bar{D}^0} t_{D^0 \bar{D}^0 \rightarrow D^0 \bar{D}^0}) \quad (13)$$

The novelty is in Eq. (13) because now we can have $K^- D^0 \bar{D}^0$ production at tree level, and this is the unity term in Eq. (13).

4 Results

First, we use the scattering matrices based on the work of [22], and we solve the Bethe–Salpeter equation in the coupled channels $D^+ D^-$, $D^0 \bar{D}^0$, $D_S^+ D_s^-$.

Fig. 10 Diagrammatic representation of the formation of the resonance R through rescattering of $D^0\bar{D}^0$ and coupling to $D^0\bar{D}^0$

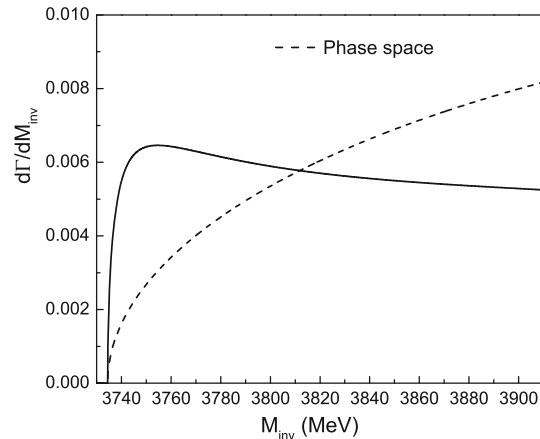
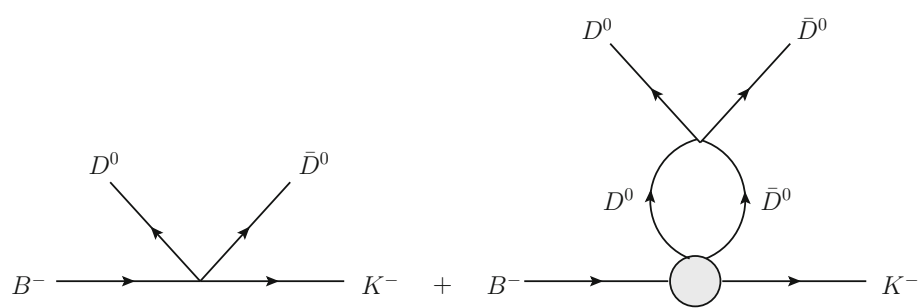


Fig. 11 The differential cross section for the reaction $\bar{B}^0 \rightarrow \bar{K}^0 D^0 \bar{D}^0$, corresponding to $V_p = 1$. The dashed line corresponds to a phase space distribution normalized to the same area in the range examined

With the $|I = 0, D\bar{D}\rangle$ wave function of Eq. (6), the $I = 0$ amplitude for $D\bar{D}$ is given by

$$t_{D\bar{D} \rightarrow D\bar{D}}^{I=0} = \frac{1}{2}(t_{11} + t_{22}) + t_{12} \quad (14)$$

where 1, 2, 3 stand for the D^+D^- , $D^0\bar{D}^0$, $D_s^+D_s^-$ channels. The coupling $g_{R, D\bar{D}}^{I=0}$ is obtained from this amplitude in the limit

$$t_{D\bar{D} \rightarrow D\bar{D}}^{I=0} \simeq \lim_{s \rightarrow M_R^2} \frac{(g_{R, D\bar{D}}^{I=0})^2}{s - M_R^2} \quad (15)$$

where M_R is the energy where the pole of the bound $D\bar{D}$ state appears.

The resonance pole at $\sqrt{s_R} = 3719.4 + i0$ MeV is obtained with no width, using the same parameters as those in [22], $\alpha = -1.3$, $\mu = 1500$ MeV.

In the following, from Eq. (10), we obtain the spectrum for the $D\bar{D}$ invariant mass distribution close to threshold in the decay of \bar{B}^0 . The differential cross section for the reaction $\bar{B}^0 \rightarrow \bar{K}^0 D^0 \bar{D}^0$ is given in Fig. 11, where the dashed line corresponds to a phase space distribution normalized to the same area in the range examined. We can see in the figure

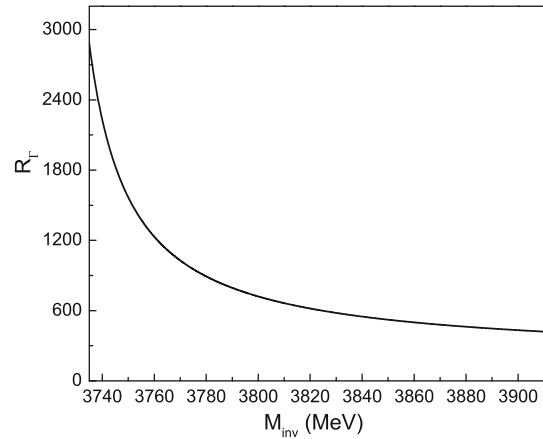


Fig. 12 Results of R_Γ of Eq. (11) as a function of $M_{\text{inv}}(D\bar{D})$ invariant mass distribution

that the shape of the $D^0\bar{D}^0$ mass distribution is quite different from phase space, and this is due to the presence of the $X(3720)$ resonance below threshold.

Next we evaluate Eq. (11) with the input of Eqs. (7) and (9), and the results are shown in Fig. 12. We observe that the ratio has some structure. There is a fall down of the ratio as a function of energy, as it would correspond to the tail of a resonance below the threshold of $D\bar{D}$, the $X(3720)$, since it is basically giving us the modulus squared of the $t_{D\bar{D} \rightarrow D\bar{D}}^{I=0}$ amplitude.

It is interesting to evaluate R_Γ because an enhancement close to threshold, as seen in Fig. 12, could in principle be due to a resonance, close to, but above threshold. However, a shape like the one in Fig. 12 is unequivocally telling us that there is a resonance below threshold. This idea has already been exploited in [46] in the $D_s^+ \rightarrow \pi^+ K^+ K^-$ reaction, by looking at the $K^+ K^-$ invariant mass distribution close to the $K\bar{K}$ threshold and dividing by the phase space factor. A shape similar to that of Fig. 12 is obtained, coming from the $f_0(980)$ resonance below the $K\bar{K}$ threshold.

Now we turn to the $B^- \rightarrow D^0\bar{D}^0 K^-$ reaction. We notice that the related experiment $B^+ \rightarrow D^0\bar{D}^0 K^+$ has already been done [38], where the $D^0\bar{D}^0$ invariant mass is measured, but with very small statistics close to threshold. In the above experiment, a sharp peak is identified which should corre-

spond to the excitation of the $\psi(3770)$ charmonium state, which decays in p-wave into $D^0\bar{D}^0$. Since the $X(3720)$ state is a scalar meson, it couples to $D^0\bar{D}^0$ in s-wave. In any case, in the work of [38], the contribution of the $\psi(3770)$ is separated and this allows us to make a comparison of our results with this distribution.

In order to compare our results with those of Ref. [38] for $B^+ \rightarrow K^+ D^0 \bar{D}^0$, we subtract from the experimental data the explicit contribution of the $\Psi(3770)$ and $D_{s1}(2700)$ which give some contribution in the region of 100 MeV above $D\bar{D}$ threshold which we study. We have taken a normalization such as to agree with that of the data and have collected events in bins of 40 MeV, integrating $d\Gamma/dM_{\text{inv}}$ on the same bins as experiment [threshold, 3750], [3750, 3790], [3790, 3830], [3830, 3870], and [3870, 3910] (units of MeV). The mass distribution $d\Gamma/dM_{\text{inv}}(D^0\bar{D}^0)$ is now given by Eq. (10) substituting $p_{\bar{K}^0}$ by p_{K^-} and $t(\bar{B}^0 \rightarrow \bar{K}^0 D^0 \bar{D}^0)$ by $t(B^- \rightarrow K^- D^0 \bar{D}^0)$ of Eq. (13). We shall come back to this after the discussion of the next section.

5 Further considerations

So far we have obtained the $X(3720)$ as a bound $D\bar{D}$ state with no width. In practice, this resonance decays into lighter pseudoscalar–pseudoscalar channels as discussed in Refs. [22, 47]. Actually, in Ref. [47] one has found that the width of the $X(3720)$ state decaying to these channels was $\Gamma = 36$ MeV and the most important decay channel was $\eta\eta$. In the present work, we do not want to go through all the coupled channels of [47] but just wish to have an idea of the effect of considering the width of the $X(3720)$ state. For this reason, we work now with four coupled channels, adding $\eta\eta$ to the former ones, D^+D^- , $D^0\bar{D}^0$, $D_s^+D_s^-$, and we introduce the transition potential $\eta\eta \rightarrow D^+D^-$, $\eta\eta \rightarrow D^0\bar{D}^0$ with a strength a (dimensionless), similar to that of the model of [47] but tuned to give $\Gamma = 36$ MeV just from the $\eta\eta$ decay channel (this is accomplished with $a = 42$).

We perform the same calculations as before, using the new $t_{D\bar{D} \rightarrow D\bar{D}}$ amplitude and the results are shown in Figs. 13 and 14. We can see that the features of the mass distribution are very similar to those obtained in the case of zero width for the $X(3720)$ state. Only the $t_{D\bar{D} \rightarrow D\bar{D}}$ matrix becomes wider in terms of the $D\bar{D}$ invariant mass and hence the enhancement of the mass distribution close to the $D\bar{D}$ threshold is not as strong as before, but clearly is different from a phase space distribution. As a consequence, the ratio of Eq. (11) is a bit softer than before, but the fall down in the invariant mass is still clear.

Finally we now look at the $B^- \rightarrow K^- D^0 \bar{D}^0$ (which we want to compare with the $B^+ \rightarrow K^+ D^0 \bar{D}^0$ data) and we show the results in Figs. 15, 16 and 17. In this case we only calculate the case with a width for the $X(3720)$. In Fig. 15

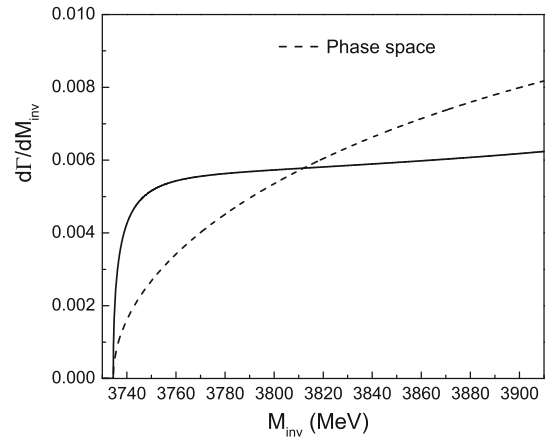


Fig. 13 The same as those in Fig. 11 but including the $\eta\eta$ channel.

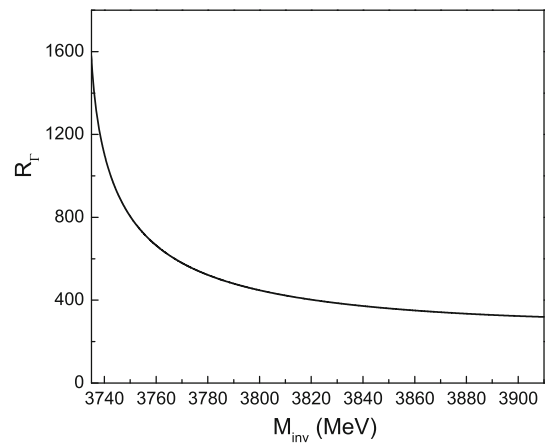


Fig. 14 The same as those in Fig. 12 but including the $\eta\eta$ channel

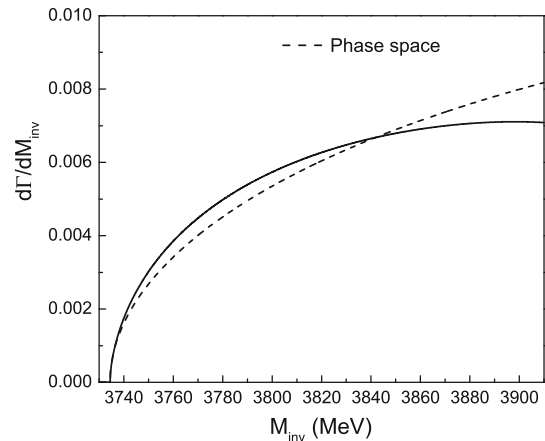


Fig. 15 The differential cross section for the reaction $B^- \rightarrow K^- D^0 \bar{D}^0$ and including the $\eta\eta$ channel. The dashed line corresponds to a phase space distribution normalized to the same area in the range examined

we show $d\Gamma/dM_{\text{inv}}$ as a function of the invariant mass. We observe in this case that there is practically no enhancement close to threshold and the distribution is closer to phase space.

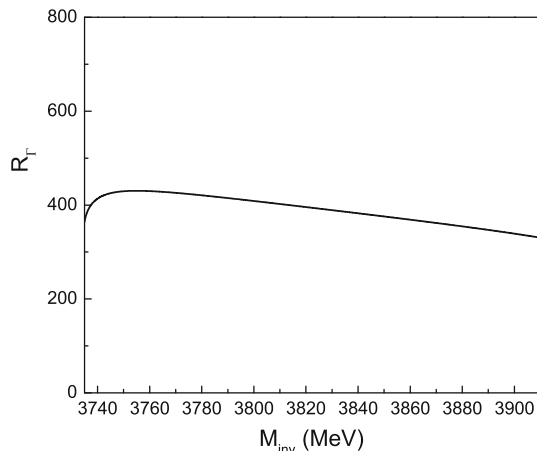


Fig. 16 Results of R_G of Eq. (11) as a function of $M_{\text{inv}}(D\bar{D})$ invariant mass distribution but for $B^- \rightarrow K^- D^0 \bar{D}^0$, including the $\eta\eta$ channel

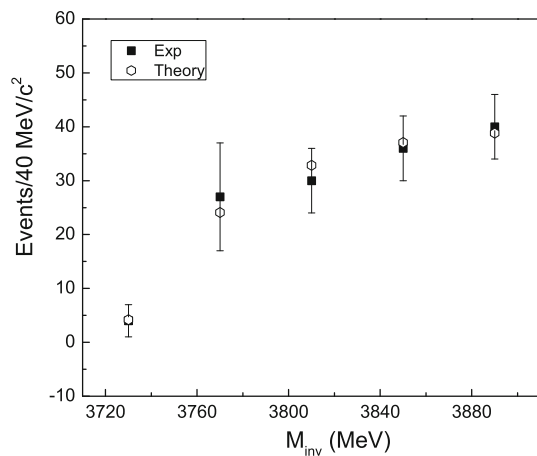


Fig. 17 Comparison between theory and experiment for the $B^- \rightarrow K^- D^0 \bar{D}^0$ decay

The reason is the term unity in Eq. (13), in contrast to Eq. (9) where only the $t_{D\bar{D}}$ matrix appears. As a consequence of this, in Fig. 16, we do not see the fall of R_G that we see in Fig. 14. In Fig. 17 we compare the mass distribution with the data of [38]. As mentioned at the end of Sect. 4, we have removed the contributions of $\psi(3770)$ and $D_{s1}(2700)$. Since these contributions come from the analysis of the data of [38], we have also taken the results for the total distribution from the same analysis, instead of the raw data. We normalize the results of Fig. 15 to the number of events in Fig. 17 and observe that, within errors, the agreement with the data is good. However, we should note that the errors are large and the bins of 40 MeV too broad. It would be most helpful to have these results improved with more statistics and better resolution. However, the message of the work is that the $B^0 \rightarrow D^0 \bar{D}^0 K^0$ decay is better suited to determine the bound state below threshold, because in this reaction we find and justify the presence of an enhancement of the $D^0 \bar{D}^0$

mass distribution close to threshold, which is due to the $D\bar{D}$ bound state.

The comparison is made here with the limited experimental information available. Further comparison of these results with coming LHCb measurements will be very valuable to make progress in our understanding of the meson–meson interaction and the nature of the scalar meson $X(3720)$.

Let us come back to the internal emission diagram of Fig. 2. This diagram is color suppressed with respect to the one of Fig. 3. Color suppression reverts into a strength of the mechanism with respect to the color favored of about one order of magnitude smaller since the mechanisms not necessarily have the same shape over the phase space. In order to estimate the relevance of that mechanism in the $B^0 \rightarrow D^0 \bar{D}^0 K^0$ process we take an upper extreme assuming the weight of the amplitude to be about 1/3 of that of Fig. 3 and adding coherently to it. The contribution of Fig. 2 is readily evaluated, the $c\bar{c}$ hadronize and we have to calculate now $(\phi\phi)_{44}$, which gives

$$(\phi\phi)_{44} = D^0 \bar{D}^0 + D^+ D^- + D_s^+ D_s^- + \eta_c \eta_c, \quad (16)$$

and we neglect the $\eta_c \eta_c$ component which will play no role here. Then, corresponding to Eq. (7), we have now

$$t'(\bar{B}^0 \rightarrow \bar{K}^0 R) = V'_P (\sqrt{2} g_{R, D\bar{D}}^{I=0} G_{D\bar{D}} + g_{R, D_s^+ D_s^-} G_{D_s^+ D_s^-}), \quad (17)$$

and corresponding to Eq. (9) we have now

$$t'(\bar{B}^0 \rightarrow \bar{K}^0 D^0 \bar{D}^0) = V'_P \left(1 + \sqrt{2} G_{D\bar{D}} t_{D\bar{D}, D\bar{D}}^{I=0} + G_{D_s^+ D_s^-} t_{D_s^+ D_s^-, D\bar{D}}^{I=0} \right), \quad (18)$$

As we have mentioned, we would take now $V'_P = V_P/3$. Adding now the amplitudes of Eqs. (7), (9), (17) and (18) we reevaluate the ratio R_G of Fig. 12. The results can be found in Fig. 18, compared to those of Fig. 12. As we can see, the changes are very small and the conclusions we drew before become more solid.

6 Conclusions

In the present paper we have studied the B^0 decay to $D^0 \bar{D}^0 K^0$ based on the chiral unitary model that generates the $X(3720)$ resonance, and we have made predictions for the $D^0 \bar{D}^0$ invariant mass distribution. From the shape of the distribution, the existence of the resonance below threshold could be induced. Additionally, we have also predicted the rate of production of the $X(3720)$ resonance to the $D^0 \bar{D}^0$

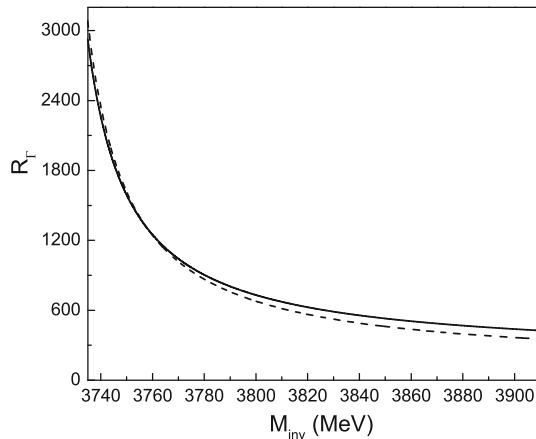


Fig. 18 The reevaluated ratio of R_Γ of Eq. (11) as a function of $M_{\text{inv}}(D\bar{D})$ invariant mass distribution. *Solid line*, as in Fig. 12. *Dashed line*, adding the contribution of the mechanism of Fig. 2 (see text)

mass distribution with no free parameters, under the assumption that the $X(3720)$ resonance is dynamically generated. So far, the related experiment $B^+ \rightarrow D^0 \bar{D}^0 K^+$ has already been done, and the $D^0 \bar{D}^0$ invariant mass is measured, but with very small statistics close to threshold, including the s-wave and p-wave parts of the spectrum. The $X(3720)$ state is a scalar meson and it decays into $D^0 \bar{D}^0$ in s-wave. In this sense, testing the invariant mass predicted here should require one to separate the s-wave from the p-wave part of the spectrum. In any case, the contribution of the $\psi(3770)$ is separated and this allows us to make a comparison of our results with this distribution.

With present errors we find a good agreement with the data. However, we found that the B^0 decay to $D^0 \bar{D}^0 K^0$ is better suited to study the $X(3720)$ resonance, since there is no tree level $D^0 \bar{D}^0$ production in this decay and this forces the $D^+ D^- \rightarrow D^0 \bar{D}^0$ transition to intervene to make $D^0 \bar{D}^0$ at the end. The implementation of the experiment in the future would be very helpful in the search of this elusive state and as a further test of the nature of the $X(3720)$ resonance.

Acknowledgments L. R. Dai would like to thank Dr. Z. F. Sun for helpful discussion. One of us, E. Oset, wishes to acknowledge support from the Chinese Academy of Science in the Program of Visiting Professorship for Senior International Scientists (Grant No. 2013T2J0012). This work is partly supported by the Spanish Ministerio de Economía y Competitividad and European FEDER funds, under the contract numbers FIS2011-28853-C02-01 and FIS2011-28853-C02-02, and the Generalitat Valenciana in the program Prometeo, 2009/090. We acknowledge the support of the European Community-Research Infrastructure Integrating Activity Study of Strongly Interacting Matter (acronym HadronPhysics3, Grant Agreement No. 283286) under the Seventh Framework Programme of EU. This work is also partly supported by the National Natural Science Foundation of China under Grant Nos. 11575076, 11375080, 11475227, and it is supported by the Program for Liaoning Excellent Talents in University (Grant No. LR2015032). It is also supported by the Open Project Program of State Key Laboratory of Theoretical Physics, Institute of Theoretical Physics, Chinese Academy of Sciences, China (Grant No. Y5KF151CJ1).

Open Access This article is distributed under the terms of the Creative Commons Attribution 4.0 International License (<http://creativecommons.org/licenses/by/4.0/>), which permits unrestricted use, distribution, and reproduction in any medium, provided you give appropriate credit to the original author(s) and the source, provide a link to the Creative Commons license, and indicate if changes were made.

Funded by SCOAP³.

References

1. E. Klemt, A. Zaitsev, Phys. Rep. **454**, 1 (2007). [arXiv:0708.4016](https://arxiv.org/abs/0708.4016) [hep-ph]
2. V. Crede, C.A. Meyer, Prog. Part. Nucl. Phys. **63**, 74 (2009). [arXiv:0812.0600](https://arxiv.org/abs/0812.0600) [hep-ex]
3. E. Oset, W.H. Liang, M. Bayar, J.J. Xie, L.R. Dai, M. Albaladejo, M. Nielsen, T. Sekihara, F. Navarra, L. Roca, M. Mai, J. Nieves, J.M. Dias, A. Feijoo, V.K. Magas, A. Ramos, K. Miyahara, T. Hyodo, D. Jido, M. Doring, R. Molina, H.X. Chen, E. Wang, L.S. Geng, N. Ikeno, P. Fernandez-Soler, Z.F. Sun, Int. J. Mod. Phys E **25**, 1630001 (2016)
4. J. Gasser, H. Leutwyler, Ann. Phys. **158**, 142 (1984)
5. J.A. Oller, E. Oset, Nucl. Phys. A **620**, 438 (1997) [Erratum-ibid. A **652**, 407 (1999)]
6. N. Kaiser, Eur. Phys. J. A **3**, 307 (1998)
7. M.P. Locher, V.E. Markushin, H.Q. Zheng, Eur. Phys. J. C **4**, 317 (1998)
8. J. Nieves, E. Ruiz Arriola, Nucl. Phys. A **679**, 57 (2000)
9. J. Nieves, E. Ruiz Arriola, Phys. Lett. B **455**, 30 (1999)
10. J.R. Pelaez, G. Rios, Phys. Rev. Lett. **97**, 242002 (2006)
11. J.R. Pelaez, [arXiv:1510.00653](https://arxiv.org/abs/1510.00653) [hep-ph]
12. J.D. Weinstein, N. Isgur, Phys. Rev. Lett. **48**, 659 (1982)
13. R. Jaffe in *The XVI International Conference on Hadron Spectroscopy* (Jefferson Lab). <https://www.jlab.org/conferences/hadron2015/index.html>. Accessed Sept 2015
14. M. Bando, T. Kugo, S. Uehara, K. Yamawaki, T. Yanagida, Phys. Rev. Lett. **54**, 1215 (1985)
15. M. Bando, T. Kugo, K. Yamawaki, Phys. Rep. **164**, 217 (1988)
16. M. Harada, K. Yamawaki, Phys. Rep. **381**, 1 (2003). [arXiv:hep-ph/0302103](https://arxiv.org/abs/hep-ph/0302103)
17. U.G. Meissner, Phys. Rep. **161**, 213 (1988)
18. C.W. Xiao, J. Nieves, E. Oset, Phys. Rev. D **88**, 056012 (2013). [arXiv:1304.5368](https://arxiv.org/abs/1304.5368) [hep-ph]
19. W.H. Liang, C.W. Xiao, E. Oset, Phys. Rev. D **89**(5), 054023 (2014). [arXiv:1401.1441](https://arxiv.org/abs/1401.1441) [hep-ph]
20. M. Neubert, Phys. Rep. **245**, 259 (1994). [arXiv:hep-ph/9306320](https://arxiv.org/abs/hep-ph/9306320)
21. A.V. Manohar, M.B. Wise, *Heavy Quark Physics, Cambridge Monographs on Particle Physics, Nuclear Physics and Cosmology*, vol. 10
22. D. Gamermann, E. Oset, D. Strottman, M.J. Vicente Vacas, Phys. Rev. D **76**, 074016 (2007). [arXiv:hep-ph/0612179](https://arxiv.org/abs/hep-ph/0612179)
23. J. Nieves, M.P. Valderrama, Phys. Rev. D **86**, 056004 (2012). [arXiv:1204.2790](https://arxiv.org/abs/1204.2790) [hep-ph]
24. C. Hidalgo-Duque, J. Nieves, M.P. Valderrama, Phys. Rev. D **87**(7), 076006 (2013). [arXiv:1210.5431](https://arxiv.org/abs/1210.5431) [hep-ph]
25. D. Gamermann, E. Oset, Eur. Phys. J. A **36**, 189 (2008). [arXiv:0712.1758](https://arxiv.org/abs/0712.1758) [hep-ph]
26. P. Pakhlov et al., Belle Collaboration, Phys. Rev. Lett. **100**, 202001 (2008). [arXiv:0708.3812](https://arxiv.org/abs/0708.3812) [hep-ex]
27. W.H. Liang, E. Oset, Phys. Lett. B **737**, 70 (2014). [arXiv:1406.7228](https://arxiv.org/abs/1406.7228) [hep-ph]
28. R. Aaij et al., LHCb Collaboration, Phys. Lett. B **698**, 115 (2011). [arXiv:1102.0206](https://arxiv.org/abs/1102.0206) [hep-ex]
29. R. Aaij et al., LHCb Collaboration, Phys. Rev. D **87**(5), 052001 (2013). [arXiv:1301.5347](https://arxiv.org/abs/1301.5347) [hep-ex]

30. J.J. Xie, L.R. Dai, E. Oset, Phys. Lett. B **742**, 363 (2015). [arXiv:1409.0401](https://arxiv.org/abs/1409.0401) [hep-ph]
31. M. Albaladejo, M. Nielsen, E. Oset, Phys. Lett. B **746**, 305 (2015). [arXiv:1501.03455](https://arxiv.org/abs/1501.03455) [hep-ph]
32. D. Gammermann, J. Nieves, E. Oset, E. Ruiz Arriola, Phys. Rev. D **81**, 014029 (2010). [arXiv:0911.4407](https://arxiv.org/abs/0911.4407) [hep-ph]
33. T. Hyodo, D. Jido, A. Hosaka, Phys. Rev. C **85**, 015201 (2012). [arXiv:1108.5524](https://arxiv.org/abs/1108.5524) [nucl-th]
34. T. Hyodo, Int. J. Mod. Phys. A **28**, 1330045 (2013). [arXiv:1310.1176](https://arxiv.org/abs/1310.1176) [hep-ph]
35. T. Sekihara, T. Hyodo, D. Jido, PTEP **2015**, 063D04 (2015). [arXiv:1411.2308](https://arxiv.org/abs/1411.2308) [hep-ph]
36. W.H. Liang, J.J. Xie, E. Oset, R. Molina, M. Dring, Eur. Phys. J. A **51**(5), 58 (2015). [arXiv:1502.02932](https://arxiv.org/abs/1502.02932) [hep-ph]
37. R. Quagliani, private communication
38. J.P. Lees et al., BaBar Collaboration, Phys. Rev. D **91**(5), 052002 (2015). [arXiv:1412.6751](https://arxiv.org/abs/1412.6751) [hep-ex]
39. S. Stone, L. Zhang, Phys. Rev. Lett. **111**(6), 062001 (2013)
40. L.L. Chau, Phys. Rep. **95**, 1 (1983)
41. L.L. Chau, H.Y. Cheng, Phys. Rev. D **36**, 137 (1987)
42. A. Bramon, A. Grau, G. Pancheri, Phys. Lett. B **283**, 416 (1992)
43. A. Martinez Torres, L.S. Geng, L.R. Dai, B.X. Sun, E. Oset, B.S. Zou, Phys. Lett. B **680**, 310 (2009). doi:10.1016/j.physletb.2009.09.003. [arXiv:0906.2963](https://arxiv.org/abs/0906.2963) [nucl-th]
44. X.-W. Kang, B. Kubis, C. Hanhart, G. Ulf, Meiner Phys. Rev. D **89**, 053015 (2014)
45. J.T. Daub, C. Hanhart, B. Kubis, JHEP **02**, 009 (2016). [arXiv:1508.06841](https://arxiv.org/abs/1508.06841) [hep-ph]
46. P. del Amo Sanchez et al., BABAR Collaboration, Phys. Rev. D **83**, 052001 (2011)
47. C.W. Xiao, E. Oset, Eur. Phys. J. A **49**, 52 (2013)